VIP The following Communications have been judged by at least two referees to be "very important papers" and will be published online at www.angewandte.org soon:

Author Profile

"My favorite reaction is the Robinson synthesis of tropinone.
I am waiting for the day when someone will discover the 30-hour day …"
This and more about Michael Willis can be found on page 1304.

News


T. Maschmeyer


J. Bremner


J. Gooding


M. Stenzel


M. Brimble


R. Payne

Books

Highlights

Organometallic Structures

Subtle differences: By using a combination of advanced crystallographic techniques and complementary computational approaches to assess the relative energies and conformational preferences, Me_2Zn has been shown to form two different crystal structures. At temperatures above 180 K the methyl groups are staggered, whereas below 180 K the methyl groups are eclipsed. In contrast, the two ethyl groups in Et_2Zn are shown to be mutually *cis*.

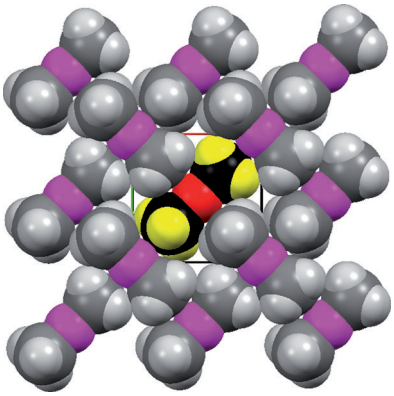

Biotechnology

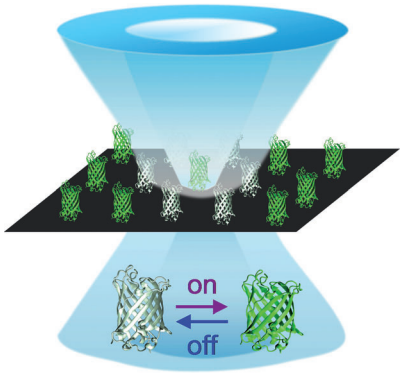

Like the battery bunny: The novel photoswitchable fluorescent protein rsEGFP can be cycled between its fluorescent and nonfluorescent states more than a thousand times and is, therefore, a superb marker for high-resolution RESOLFT imaging (RESOLFT = reversible saturable optical fluorescence transition) and data storage applications.

Reviews

Artificial Aptamers

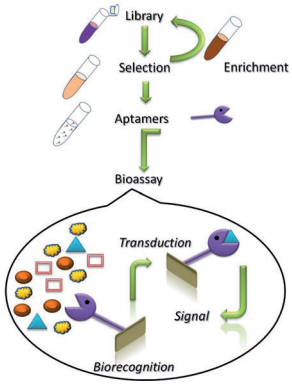

Antibody alternatives: This Review covers the peculiarities of the two major classes of affinity molecules produced by evolutionary approaches: nucleic acid aptamers and combinatorial non-immunoglobulin proteins (termed here, for convenience, simply peptide aptamers). The applications of these molecules in the bioanalytical field are discussed.

For the USA and Canada:
ANGEWANDTE CHEMIE International Edition (ISSN 1433-7851) is published weekly by Wiley-VCH, PO Box 191161, 69451 Weinheim, Germany. Air freight and mailing in the USA by Publications Expediting Inc., 200 Meacham Ave., Elmont, NY 11003. Periodicals postage paid at Jamaica, NY 11431. US POSTMASTER: send address changes to *Angewandte Chemie*, Journal Customer Services, John Wiley & Sons Inc., 350 Main St., Malden, MA 02148-5020. Annual subscription price for institutions: US$ 11.738/10.206 (valid for print and electronic / print or electronic delivery); for individuals who are personal members of a national chemical society prices are available on request. Postage and handling charges included. All prices are subject to local VAT/sales tax.

Communications

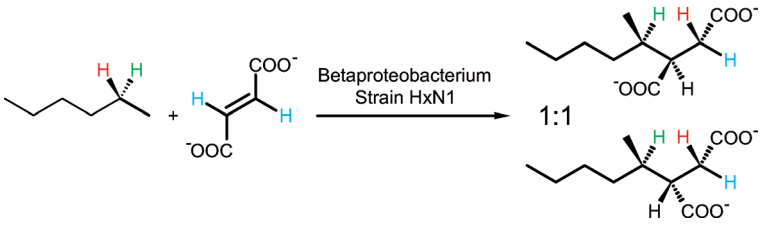

Anaerobic growth of the bacterium strain HxN1 with *n*-hexane gives nearly equal amounts of (2*R*,1′*R*)- and (2*S*,1′*R*)-(1-methylpentyl)succinate, which are formed by the radical addition of the hydrocarbon to fumarate (see scheme). The highly selective attack on the pro-*S* hydrogen atom at C2 of *n*-hexane is associated with inversion of the configuration at C2 during binding to fumarate and exhibits isotopic discrimination against a C—^{2}H bond.

Alkane Activation

Made by the barrel load: The biosynthetic pathway of the recently discovered 22nd amino acid, pyrrolysine, starts with an isomerization of lysine to methylornithine, catalyzed by PylB. The X-ray crystal structure of PylB is determined (see picture) and shows it has a TIM barrel fold. The sealed central cavity contains a [4Fe-4S] cluster, *S*-adenosylmethionine (SAM), and methylornithine, whose 2*R*,3*R* configuration could be confirmed. The data suggest a fragmentation–recombination mechanism via a glycyl radical intermediate.

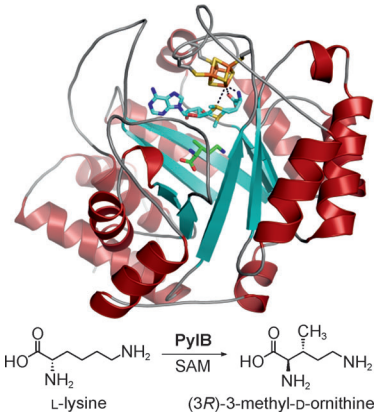

Pyrrolysine Biosynthesis

Pore relations: Reagent molecules form head-to-tail chains in the pores of ZSM-5 zeolite particles in the presence or absence of acidic sites, according to multiplex coherent anti-Stokes Raman scattering spectromicroscopy (mCARS). The molecular ordering in the pores makes it possible to characterize the crystallographic subunits of individual ZSM-5 particles with (sub)micrometer spatial resolution in three dimensions.

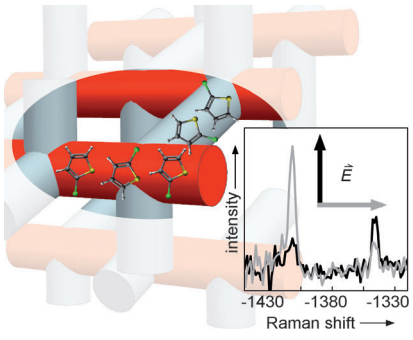

Zeolite Imaging

Kaolinite-Based Janus Particles

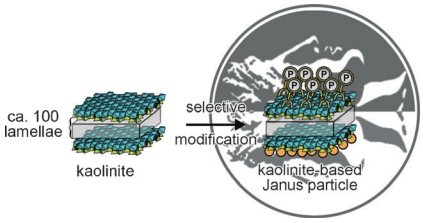

Kaolinite platelets have inherent Janus character owing to a polar crystal structure. This character is, however, ineffective without selective modification of the two hydrophilic external basal surfaces. Amplification of the difference in the chemical nature of the surfaces is achieved by cation exchange on one side and by covalent grafting on the other. After adjustment of the surface tension, kaolinite is an effective emulsifier.

Ambident Reactivity

Kinetics versus thermodynamics: Methyl groups increase the nucleophilic reactivity of the substituted position of hydrazines and reduce the nucleophilicity of the adjacent nitrogen center. As a result, the tertiary nitrogen atom of 1,1-dimethylhydrazine is 3000 times more reactive than the NH_2 group, but under thermodynamic control substitution of an NH_2 proton occurs (see picture).

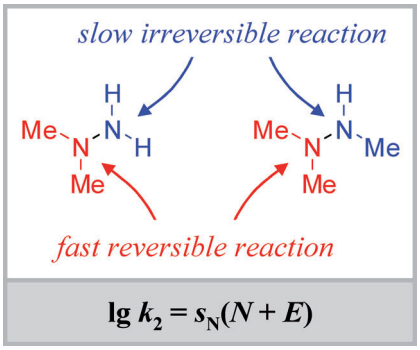

Iron Catalysis

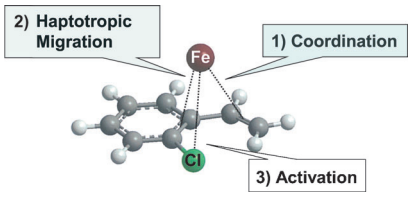

An effective protocol for iron-catalyzed biaryl syntheses by coupling chlorostyrenes with aryl Grignard reagents requires only mild reaction conditions and tolerates various functional groups. The underlying activation of deactivated aryl chlorides proceeds through a rate-determining coordination of the catalyst to the vinyl substituent and subsequent haptotropic migration along the conjugated π system to the site of C–Cl bond cleavage.

Drug Design

Irradiation makes the difference: The relaxation-rate differences of individual ligand protons (H_A, H_B) between the experiment with (see picture, red) and that without (blue) saturation of the protons of the protein target reflect the proximity to the protein surface. Thus, the binding portions of ligand molecules could be identified using this "difference of inversion recovery rate with and without target irradiation" (DIRECTION) method.

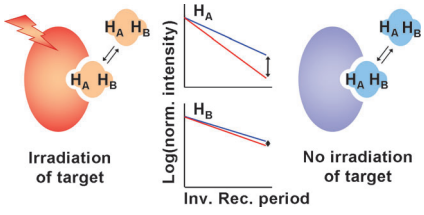

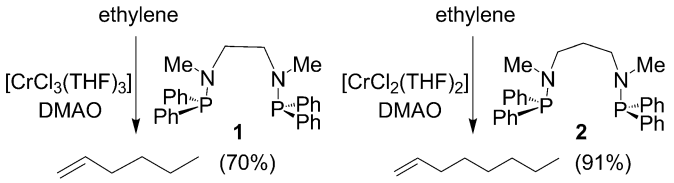

Small change, big difference: The introduction of an additional CH_2 group into the bridge of ligands with two P/N units leads to a different selectivity of the corresponding chromium-based catalysts. Whereas **1** produces an ethylene trimerization system, **2** provides an unprecedented ethylene tetramerization system that produces 1-octene with high purity and little or no polymer side products (see scheme; DMAO = Me_3Al-depleted methylaluminoxane).

Ethylene Tetramerization

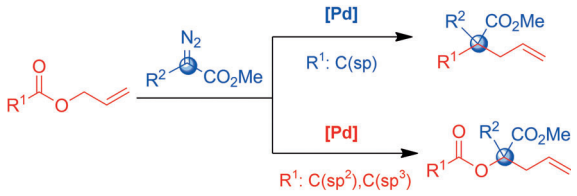

Take two: α-Diazocarbonyl compounds display a diverse pattern of reactivity upon palladium-catalyzed reaction with esters. Esters bearing an alkynyl group on the carbonyl carbon atom lead to two different C–C bonds at the same carbon atom in a single operation through decarboxylation and migratory insertion, whereas aromatic and benzylic acid derivatives afford aromatic and benzylic esters bearing an O-substituted quaternary carbon center.

Palladium Catalysis

Accurate structural information: The first high-resolution study of isolated gas-phase acetyl salicylic acid (aspirin) is reported. Solid aspirin was vaporized by laser ablation, expanded in a supersonic jet, and characterized by Fourier transform microwave spectroscopy (see picture). Two different neutral structures have been identified from the analysis of the rotational spectrum.

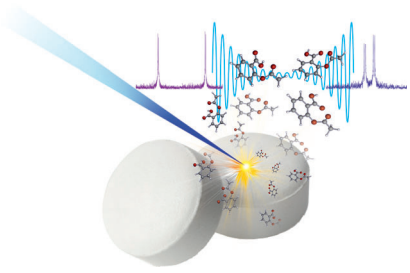

Gas-Phase Conformations

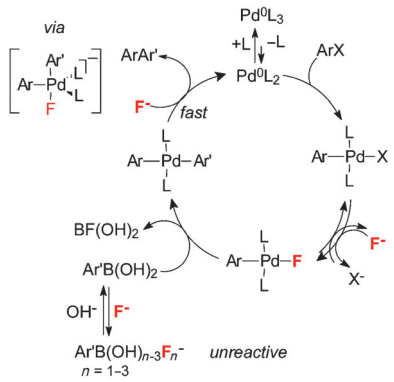

Fluoride ions play three roles in the Suzuki–Miyaura reaction. They favor the reaction by formation of *trans*-[ArPdF(PPh_3)$_2$], which reacts with Ar′B(OH)$_2$ in an unprecedented rate-determining transmetalation, and by promoting the reductive elimination from the *trans*-[ArPdAr′(PPh_3)$_2$] intermediate. Conversely, F^- disfavors the reaction by formation of unreactive anionic Ar′B(OH)$_{n-3}F_n^-$ ($n = 1–3$), leading to two antagonistic effects of F^- in the transmetalation.

Suzuki–Miyaura Reactions

Catalytic Transamidation

Transamidation of Primary Amides with Amines Using Hydroxylamine Hydrochloride as an Inorganic Catalyst

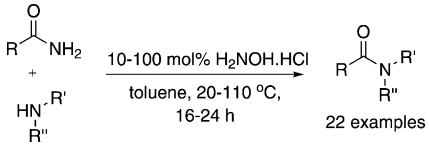

Metal-free catalysis: A method for the transamidation of primary amides with primary or secondary amines provides access to secondary and tertiary amides, by utilizing catalytic quantities of hydroxylamine hydrochloride to activate the chemically robust primary amide group (see scheme). A mechanism of primary amide activation through a hydrogen-bonding complex is proposed.

Biomass Conversion

Production of Renewable Aromatic Compounds by Catalytic Fast Pyrolysis of Lignocellulosic Biomass with Bifunctional Ga/ZSM-5 Catalysts

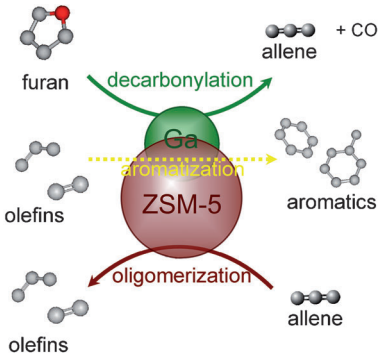

Burn, baby, burn! A new bifunctional catalyst (Ga/ZSM-5) displays increased selectivity for the production of aromatic compounds during the catalytic fast pyrolysis of biomass. With this Ga-promoted ZSM-5 catalyst, olefins such as ethylene and propylene, which are produced as intermediates, are more efficiently converted into aromatic compounds, especially benzene. Ga/ZSM-5 also promotes decarbonylation and olefin-aromatization reactions.

Asymmetric Propargylation

Brønsted Acid Catalyzed Asymmetric Propargylation of Aldehydes

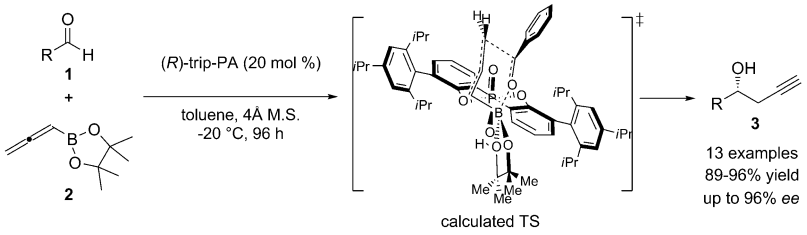

Which gets activated? A versatile and highly enantioselective chiral Brønsted acid catalyzed method for the propargylation of aldehydes is described to provide a range of chiral homopropargylic alcohols. Computational studies support the belief that the chiral phosphoric acid activates the allenyl boronic acid pinacol ester reagent rather than the aldehyde.

Helical Peptides

Induction of Unexpected Left-Handed Helicity by an N-Terminal L-Amino Acid in an Otherwise Achiral Peptide Chain

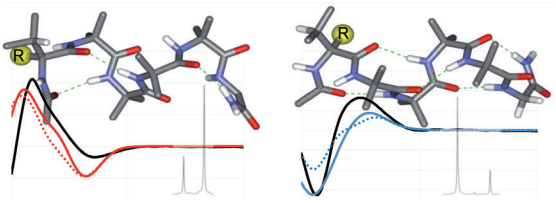

Peptide helices containing L-amino acids are typically right-handed. Exceptions are peptide helices containing the achiral amino acids 2-aminoisobutyric acid and glycine with a single chiral amino acid at the N terminus. These helices are left-handed when the N-terminal residue is a common tertiary proteinogenic amino acid, such as L-valine (see picture, left), but right-handed when the N-terminal residue is the quaternary amino acid L-α-methylvaline (right).

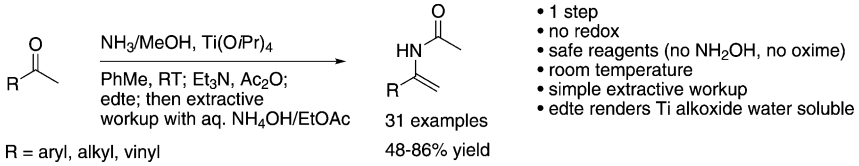

A one-step conversion of ketones into *N*-acetyl enamides was developed. The process employs safe and inexpensive reagents, proceeds under mild conditions, and tolerates diverse functional groups. The addition of edte (*N*,*N*,*N*′,*N*′-tetrakis(2-hydroxyethyl)ethylenediamine) prior to workup enables water solubilization of Ti alkoxides and allows a simple extractive workup.

Enamide Synthesis

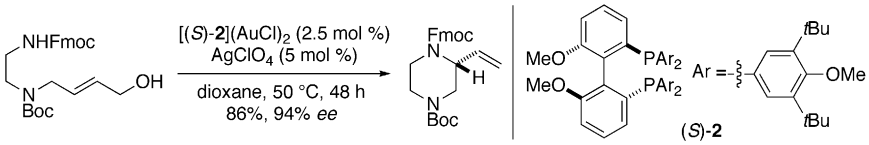

Aliphatic nitrogen heterocycles—either five- or six-membered—are formed in high yield and with up to 94% *ee* when a 1:2 mixture of [(*S*)-**2**](AuCl)$_2$ and $AgClO_4$ is used as the catalyst for the title reaction.

Allylic Amination

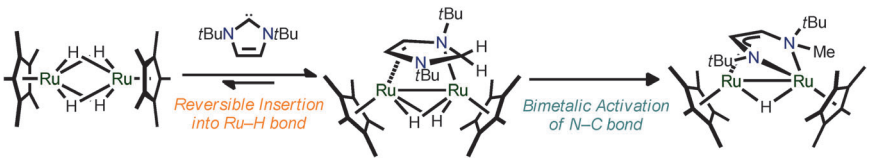

Reversible insertion of NHC: 1,3-Di-*tert*-butylimidazol-2-ylidene was inserted into a ruthenium–hydride bond of [Cp*Ru(μ-H)$_4$RuCp*] to form a 4-imidazoline complex that underwent a dynamic process, namely 1,3-migratory pendulum motion of the 4-imidazoline ligand (see scheme). Bimetallic-system-assisted N–C bond cleavage of the imidazoline ligand proceeded to generate a pseudo-diazaruthenacycle.

NHC Ligands

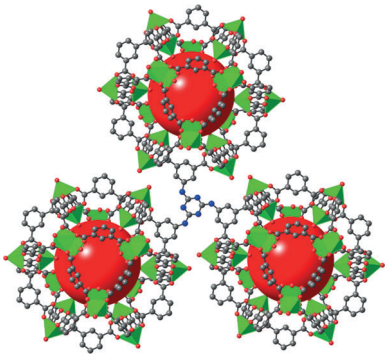

Open and friendly: The smallest member of the *rht*-type metal–organic frameworks (MOFs, see picture) constructed by a hexacarboxylate ligand with a nitrogen-rich imino triazine backbone shows a significantly enhanced gas binding affinity relative to all other isoreticular *rht*-type MOFs. The high adsorption capacity and remarkable selectivity of CO_2 are attributed to the high density of open metal and Lewis basic sites in the framework.

Metal–Organic Frameworks

Stability of DNA

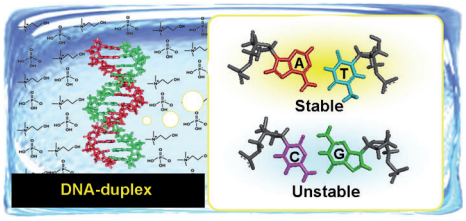

A green solvent: Quantitative thermodynamic analyses shows that A–T base pairs are more stable than G–C base pairs in the hydrated ionic-liquid choline dihydrogen-phosphate because of specific interactions between DNA bases and choline ions.

Microcapsules

Soft origami structures: Planar bilayer microparticles consisting of active and passive layers show a structural transformation to microcapsules because of an anisotropic volume expansion (see picture). The soft hydrogel materials used for both layers facilitate the reversible transformation and complete closure of the compartment, which enables in situ encapsulation and triggered release of micro- to nanoscopic active ingredients.

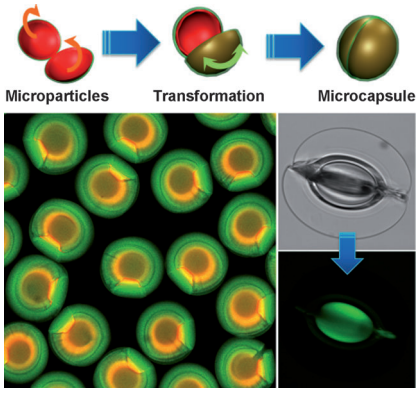

Nanoparticles

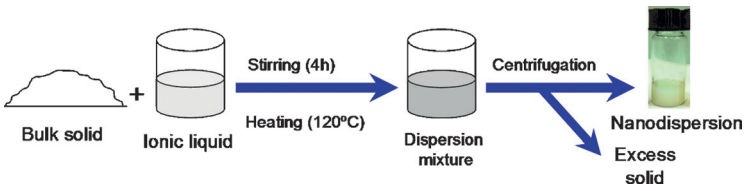

Just add liquid and stir: Dispersions of metal sulfide nanoparticles (CdS, ZnS, PbS, and MnS) can be prepared directly by mixing the corresponding bulk solid with an appropriate ionic liquid, without further additives or solvents (see scheme). The selection of the ionic liquid is critical for the viability of this nanoparticle preparation method.

Fluid Catalytic Cracking

Cracking the crackers: Integrated laser and electron microscopy was applied to study individual fluid catalytic cracking catalyst particles (see picture) deactivated according to an industrially relevant protocol. New insights have been obtained by correlating Brønsted acidity changes, visualized using fluorescence microscopy, with structural transformations in the zeolite and matrix components, as observed with electron microscopy.

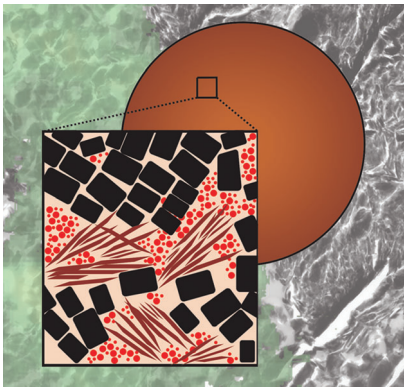

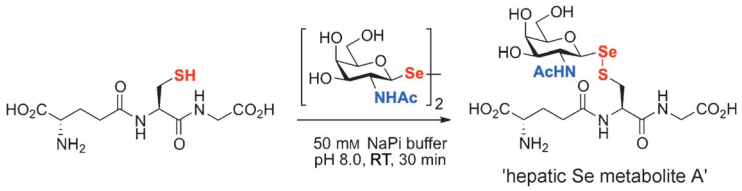

Introducing selenium: The synthesis and full characterization of human hepatic Se metabolite A has been accomplished by using a robust, efficient, and Cys-specific selenenylation protocol (see scheme; NaPi = sodium phosphate). The selenenylsulfide linkage is sufficiently stable to allow quantification of Se-containing glycoconjugates in biological fluids by using atomic detection methods.

Metabolites

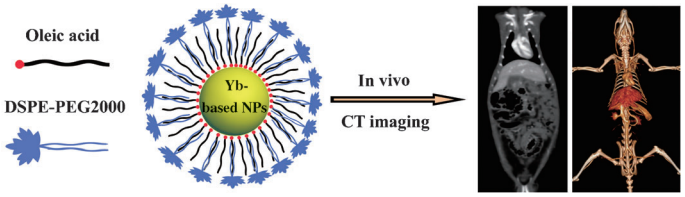

Enlightening particles: A contrast agent for in vivo X-ray computed tomography (CT) imaging is composed of an Yb-based nanoparticle (NP) that is stabilized with oleic acid and modified with the biocompatible polymer DSPE-PEG 2000 (see picture). The contrast agent exhibits long circulation time in vivo and low toxicity and is also much more effective than a clinical iodinated agent.

Imaging Agents

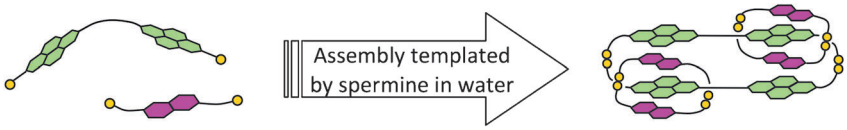

Three rings: The self-assembly of a water-soluble [3]catenane from a library composed of two linear building blocks, both terminated by cysteine components, is promoted either by a high salt concentration or by the presence of spermine. The spermine-templated synthesis of the [3]catenane shows that such structures can exhibit strong binding interactions with a biologically relevant target in water under near-physiological conditions.

Catenanes

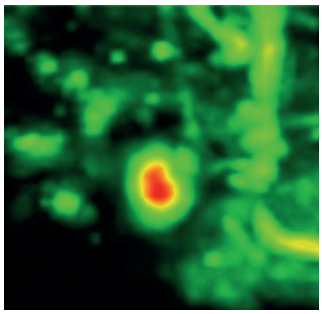

Skin-deep: The combination of a near-infrared fluorescent protein (iRFP) and deep-tissue photoacoustic tomography clearly demonstrates the superiority of iRFP over other genetically encoded probes. Impressive resolution (280 μm lateral and 75 μm axial) was obtained at a depth of 4 mm in a live animal, and volumetric images of a tumor were produced (see image), thus allowing the spatially resolved monitoring of its development.

Imaging Agents

Molecular Capsules

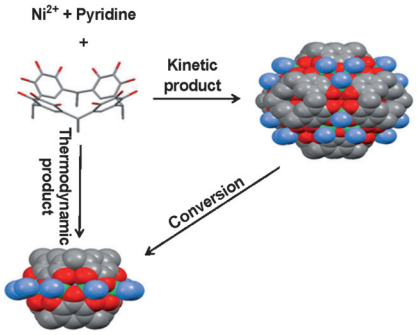

Thermodynamic versus kinetic control: Small-angle neutron scattering (SANS) and single-crystal X-ray diffraction data have been used to elucidate the effect of temperature, solvent, and metal identity on the formation of dimeric or hexameric metal-seamed pyrogallol[4]arene capsules. Higher temperatures, methanol solution, and the use of nickel metal favor dimer formation (see scheme).

C–H Activation

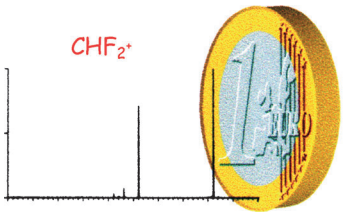

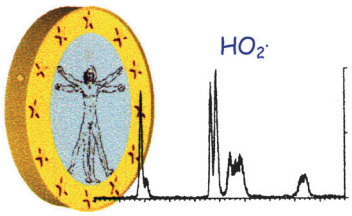

The flip side: Both the charged and uncharged products formed by C–H bond electrophilic activation have been experimentally detected in the gas phase. The $HO_2^{\bullet}$ radical is formed by a process involving the prototypical oxygen-centered radical cation $O_2^{\bullet+}$ and the methane derivative CH_2F_2.

Mesoporous Materials

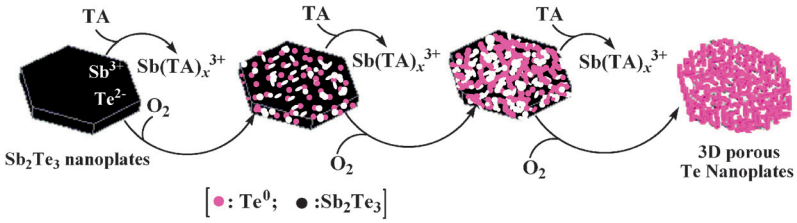

Pore genius: Sb_2Te_3 hexagonal nanoplates can be transformed into 3D porous network-structured Te plates by the dissolution of Sb^{3+} ions induced by tartaric acid (TA), the O_2-assisted oxidation of Te^{2-} ions to Te^0, and a subsequent Ostwald ripening process (see picture). These Te plates can be adopted as templates for the synthesis of 3D porous nanothread-based (or nanotube-based) metal and metal telluride nanoplates.

Stereochemistry

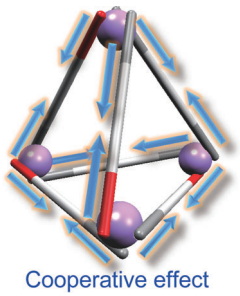

One for all, all for one: A self-assembled M_4L_6 cage, incorporating small amounts of enantiopure subcomponents at the peripheries, forms predominantly with a one-handed twist at all metal centers. Strong stereochemical coupling between metal centers in the cage amplifies energy differences between the ΔΔΔΔ and ΛΛΛΛ diastereomers as compared to analogous mononuclear metal complexes (see picture; red and gray bars denote chiral and achiral subcomponents, respectively).

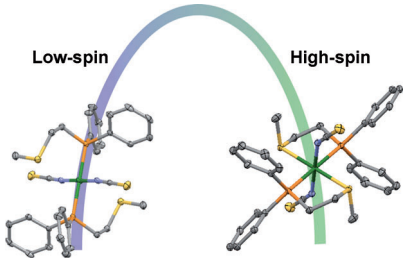

Freeze-frame: Octahedral and square-planar structural isomers, representing the two "end states" in a hemilabile ligand bond-breaking isomerization reaction, have been characterized in solution by spectroscopic methods and in the solid state by X-ray crystallography (see picture: Ni green, C gray, P orange, N blue, S yellow).

Coordination Chemistry

Networking: A bisporphyrin compound possessing an electron-deficient guest moiety assembles in a head-to-tail manner to form polymeric aggregates. Diffusion-ordered NMR spectroscopy and viscosity measurements of the aggregates confirmed the formation of sizable supramolecular polymers. Widely spread nanonetworks (see picture) are formed in solid state.

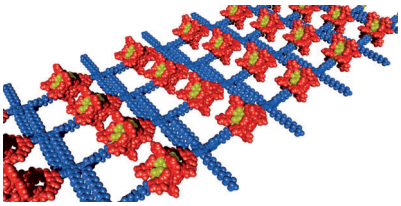

Supramolecular Polymers

New C-based ligands? Inspired by recent work on main group allotropes, a theoretical examination of Lewis base (NHC, phosphine) stabilized dicarbon has been carried out. The results indicate that the phosphine and NHC adducts of C_2 have significantly different electronic structures and that both types of molecules should be powerful, bifunctional carbon-based ligands.

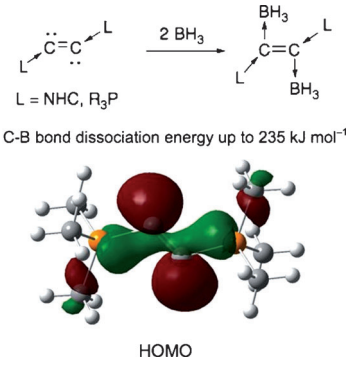

Dicarbon

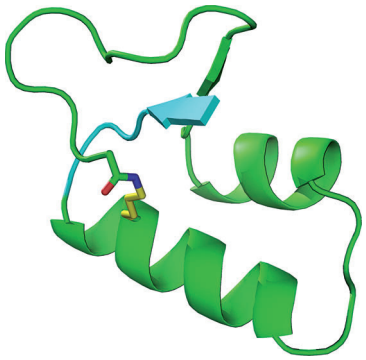

Lassoed at the other end: Original synthetic and structure determination methods were used to make a protein molecule with an unprecedented linear-loop polypeptide chain topology, and to characterize its X-ray structure.

Protein Topology

Supporting information is available on www.angewandte.org (see article for access details).

A video clip is available as Supporting Information on www.angewandte.org (see article for access details).

This article is available online free of charge (Open Access)

This article is accompanied by a cover picture (front or back cover, and inside or outside).

Service

Angewandte Corrigendum

Mesoporous Silica with Site-Isolated Amine and Phosphotungstic Acid Groups: A Solid Catalyst with Tunable Antagonistic Functions for One-Pot Tandem Reactions

N. R. Shiju,* A. H. Alberts, S. Khalid, D. R. Brown, G. Rothenberg* ——— **9615–9619**

Angew. Chem. Int. Ed. **2011**, *50*

DOI: 10.1002/anie.201101449

In this Communication, extra citations are added to reference [4] as follows:

[4] x) A. Kuschel, M. Drescher, T. Kuschel, S. Polarz, *Chem. Mater.* **2010**, *22*, 1472; y) S. Shylesh, A. Wagener, A. Seifert, S. Ernst, W. R. Thiel, *Angew. Chem.* **2010**, *122*, 188; *Angew. Chem. Int. Ed.* **2010**, *49*, 184.